International Journal of Engineering Research
Volume No.4, Issue No.11, pp : 586-591
ISSN:2319-6890)(online),2347-5013(print)
01 Nov. 2015

Sub-Harmonics in Wind Driven SM-DFIG in the Super-Synchronous Range of Operation

Mahmoud A. Saleh, Mona N. Eskander, Maged N. F. Nashed
Electronics Research Institute, Cairo, Egypt
mahmoudsaleh36@yahoo.com , eskander@eri.sci.eg , maged@eri.sci.eg

Abstract: ***In this paper the sub-harmonics associated with a specially designed single machine brushless doubly fed induction generator (SM-BDFIG) are analyzed at super-synchronous speeds. The SM-BDFIG is coupled to a variable speed wind turbine, and its rotor circuit is connected to a 3-phase rectifier feeding Li-ion batteries. A mathematical model, using Fourier expansion, is developed to define the sub-harmonics created by the time harmonics of the rotor currents irrespective of any other space or time harmonics due to winding distribution, unbalanced grid phases, or presence of harmonics in the grid voltages. The effect of the positive and negative sequence harmonics on the performance of the generator is then presented, showing the speed ranges within which these sub-harmonics are most effective, as well as the speed ranges within which these sub-harmonics are least effective. The obtained results help to design a SM-BDFIG with less harmonic distortion, hence improving its performance in wind energy conversion systems.***

Keywords: Single Machine Brushless Doubly-Fed Induction Generator "SM-BDFIG", 3-phase bridge converter, Sub-harmonics, Battery charge, and DC link.

I. Introduction

Wind energy technologies has been steadily decreasing costs and increasing efficiency to the extent that wind technologies in many cases can now be cost competitive with other sources (fossil fuel or hydro power), without any subsides. Wind energy conversion systems (WECS) growth is increasingly driven by its competitive pricing and through the need to address the choking smog that is increasingly making major urban areas in the developing and developed countries unlivable. The need for clean, sustainable, indigenous source of energy is gradually being met through renewable energy technologies and specially wind technologies.
Newly manufactured WECS are using mainly Doubly Fed Induction Generators (DFIG) due to their well known merits. It is expected that in the near future the Brushless Doubly Fed Induction Generators (BDFIG) will replace the DFIG to avoid the drawbacks of the presence of the DFIG brushes. Among the different types of BDFIG [i-ix], the Single Machine Brushless Doubly Output Induction Generators (SM-BDFIG) proposed in [i] is expected to find wide-spread utilization. The main concern in this paper to investigate the sub-harmonics created in the terminal voltage of the SM-BDFIG due to the rotor current harmonics in the super synchronous mode of operation. This investigation applies also to any DFIG having a rotor circuit connected to six-IGBT converter.
Harmonics of DFIG were investigated in previous publications [x-xiv]. In [x], the effect of the low-frequency harmonics of the rotor side of a DFIG on the stator currents and voltages was analyzed for small and medium–sized generators. In [xi] the effect of system harmonics and unbalanced voltages in a network as applied to the operation of a doubly fed induction wind generator was studied from magnetic view without recommendations to improve the harmonics effects. In [xii], the authors presented a systematic method to analyze the harmonics caused by non-sinusoidal rotor injection and unbalanced stator conditions in a DFIG using equivalent circuits. However, details of the most effective sub-harmonics were not given. In [xiii] the authors presented a power electronic interface with harmonic filters to reduce the total harmonic distortion (THD) and enhance power quality during disturbances for a WECS employing DFIG. Also, detailed harmonic analysis was not investigated. In [xiv], a stator current harmonic suppression method using a sixth-order resonant controller to eliminate negative sequence fifth- and positive sequence seventh-order current harmonics was proposed. These harmonics were due to unbalance in the grid for WECS employing DFIG. The effects of rotor harmonics were not considered.
This paper is concerned with the sub-harmonics created by the time harmonics of the rotor currents irrespective of any other space or time harmonics due to winding distribution, unbalanced grid phases, or presence of harmonics in the grid voltages.

II. Sub-harmonics fields created by the rotor harmonic currents

The SM-BDFIG [i] is designed such that the main generator, the converter, and the battery pack are all mounted on the same shaft. The layout of the SM-BDFIG rotor is shown in Fig. (1). The rotor winding is connected to six-IGBT converter. In the super-synchronous range of operation, the wave forms of the currents in the different rotor phases (a, b, c) are as shown in Fig. (2). These currents are expressed using Fourier expansion as follows:

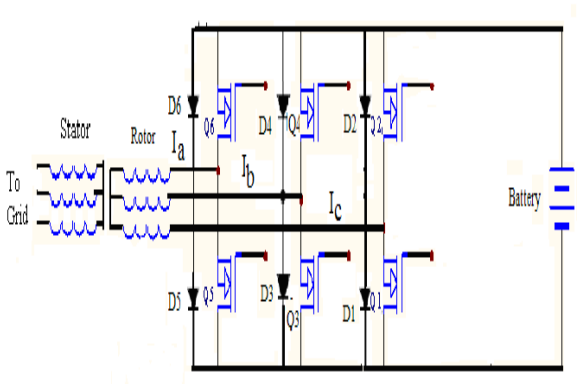

Figure (1) Layout of SM-BDFIG

ISSN:2319-6890)(online),2347-5013(print)
01 Nov. 2015

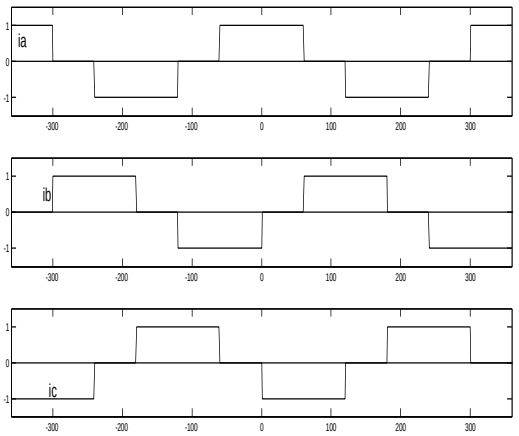

Figure (2) Wave forms of the currents in different phases.

$$i_a = I_f[\cos\alpha - \sum_{k=1}^{\infty}\frac{1}{6k-1}\cos(6k-1)\alpha + \sum_{k=1}^{\infty}\frac{1}{6k+1}\cos(6k+1)\alpha] \quad (1)$$

$$i_b = I_f[\cos(\alpha-\frac{2\pi}{3}) - \sum_{k=1}^{\infty}\frac{1}{6k-1}\cos(6k-1)(\alpha-\frac{2\pi}{3}) + \sum_{k=1}^{\infty}\frac{1}{6k+1}\cos(6k+1)(\alpha-\frac{2\pi}{3})]$$

$$= I_f[\cos(\alpha-\frac{2\pi}{3}) - \sum_{k=1}^{\infty}\frac{1}{6k-1}\cos((6k-1)\alpha+\frac{2\pi}{3})) + \sum_{k=1}^{\infty}\frac{1}{6k+1}\cos((6k+1)\alpha-\frac{2\pi}{3}))] \quad (2)$$

$$i_c = I_f[\cos(\alpha-\frac{4\pi}{3}) - \sum_{k=1}^{\infty}\frac{1}{6k-1}\cos((6k-1)\alpha+\frac{4\pi}{3})) + \sum_{k=1}^{\infty}\frac{1}{6k+1}\cos((6k+1)\alpha-\frac{4\pi}{3}))] \quad (3)$$

Where I_f = maximum value of the fundamental component of rotor current

α= s.p.ω.t

s=slip = $\frac{\omega_s - \omega}{\omega_s}$

ω_s = synchronous angular speed of the generator equal to the angular rotating speed of the fundamental component of the magnetic field in space

ω = rotor angular speed

p =number of generator pole pairs

t = time in seconds

The equations (1), (2), and (3) show that the fundamental component and the (6k+1) harmonic components have the same phase sequence i_a-i_b-i_c known as the positive sequence group.

The (6k-1) harmonic components, as indicated in equations (1), (2), and (3) have a negative phase sequence i_a-i_c-i_b.

The positive sequence harmonic currents flowing in the rotor winding will create rotating harmonic magneto-motive force (MMF) and consequently harmonic magnetic fields. The MMF wave created by the positive sequence harmonic currents will be rotating with an angular speed $s\omega_s = \omega_s - \omega$ with respect to the rotor. Since the super-synchronous range of operation is considered, i.e. $\omega > \omega_s$, then the positive sequence MMF wave (field) will rotate with a speed of (6k+1) (ω-ω_s) with respect to the rotor, and in opposite direction to the rotor speed. Naturally, the negative sequence MMF wave will rotate with a speed (6k-1) (ω-ω_s) relative to the rotor and in the same direction.

The speed of the rotating fields in space created by the positive sequence harmonic currents will be:

$$\omega_h = \omega - (6k+1)(\omega - \omega_s) \quad (4)$$

Where ω_h is the angular speed of the sub-harmonic field in space. Equation (4) can be written as:

$\nu_h = \nu - (6k+1).(\nu-1)$

$$\nu_h = (6k+1) - 6k\nu \quad (5)$$

Where, ν is the per unit angular speed of the rotor = ω / ω_s

ν_h is the per unit angular speed of the sub-harmonic field in space = ω_h / ω_s

The negative sequence harmonic rotor currents will create MMF waves or magnetic fields rotating in space with a speed equal to:

$\omega_h = \omega + (6k-1)(\omega - \omega_s) = 6k\omega + (6k-1)$

$$\text{Hence, } \nu_h = 6k\nu - (6k-1) \quad (6)$$

The "per unit angular speed" of the sub-harmonic field in space is at the same time the sub-harmonic "order". The sub-harmonic order is not necessarily multiple of the fundamental component (second, third, fifth,..) but is in most cases a fraction of the fundamental component , such as one tenth, twelve tenth, twenty three tenth,…, i.e. 0.1,1.2,2.3,..etc.

The variations of the sub-harmonic speed ν_h with the rotor angular speed ν (within the range $1.3 > \nu > 1$) are shown in Fig. (3) for the sub-harmonic fields created by the 7th and 13th rotor harmonic currents (positive sequence group). Figure (4) shows the same variations of the sub-harmonic fields created by the 5th and 11th order rotor harmonic currents. It is clear from Fig. (3) that the 7th rotor harmonic current creates, in the considered range of rotor angular speed, sub-harmonic fields rotating in space with per unit speeds less than unity. These sub-harmonics rotate in the same direction of the rotor in the speed range $1.16 > \nu > 1$, while these sub-harmonics rotate in the opposite direction of the rotor in the speed range $1.3 > \nu > 1.16$. The same behaviour exists for the 13th sub-harmonic rotor current, but in different ranges of rotor speed, i.e. $(1.09 > \nu > 1)$, and $(1.3 > \nu > 1.09)$, and in different limits of the sub-harmonic speed $(1 > \nu > -2.6)$.

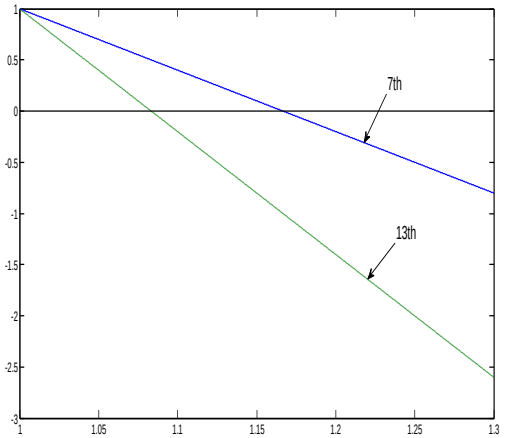

Figure (3) Sub-harmonic fields per unit speed in space (order) versus rotor angular per unit speed created by positive sequence rotor harmonic (7th & 13th) currents.

ISSN:2319-6890)(online),2347-5013(print)
01 Nov. 2015

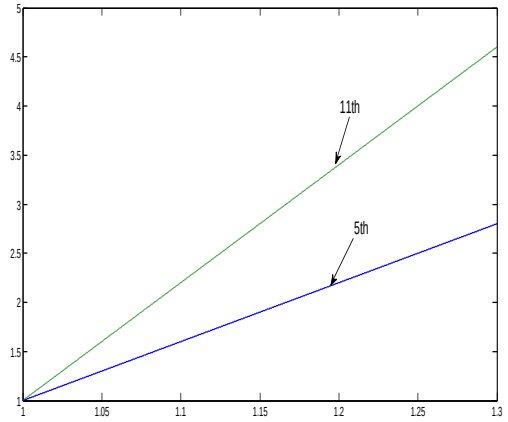

Figure (4) Sub-harmonic fields per unit speed in space (order) versus rotor angular per unit speed created by negative sequence rotor harmonic (5^{th} & 11^{th}) currents.

Figure (4) shows the variation of the speeds of the sub-harmonics created by the 5^{th} and 11^{th} harmonic rotor currents within the same range of the rotor speed. In this case the sub-harmonic field rotates in the same direction as the rotor (ν_h is positive) within the whole range of the rotor speed, ($1.3 > \nu > 1$). The speed range of the sub-harmonic fields created by the 5^{th} harmonic rotor current lies within ($2.8 > \nu > 1$), while those created by the 11^{th} harmonic rotor current is in the range of ($4.6 > \nu > 1$).

III. Voltages induced in the stator by the sub-harmonic fields

Each sub-harmonic field will induce in the stator winding an electromotive force (E_h) whose magnitude is proportional to the angular speed of the sub-harmonic field in space multiplied by the magnitude of the harmonic rotor current producing it. Therefore, the ratio of the sub-harmonic e.m.f. (E_h) to that induced by the fundamental component (E_1) is given from equations (1) and (5) for the positive sequence group as:

$$\frac{E_h}{E_1} = \frac{1}{6k-1}[(6k+1) - 6k\gamma] \qquad (7)$$

and for the negative sequence group as:

$$\frac{E_h}{E_1} = \frac{1}{6k-1}[6k\gamma + (6k-1)] \qquad (8)$$

Where k=1, 2,…and (6k±1) is the order of the harmonic rotor currents creating the sub-harmonic fields.

The ratio E_h/E_1 for different harmonic rotor currents (7^{th}, 13^{th}, 5^{th}, and 11^{th}) are shown in Figs. (5) and. (6). The shown ratio is that of absolute values irrespective of the sign of ν_h, i.e. irrespective of the direction of rotation of the sub-harmonic fields.

From Figs. (5) and (6) it is clear that the induced voltages from the positive sequence harmonics (7^{th}, 13^{th}) are much smaller than those induced by the negative sequence harmonic currents (5^{th}, 11^{th}).

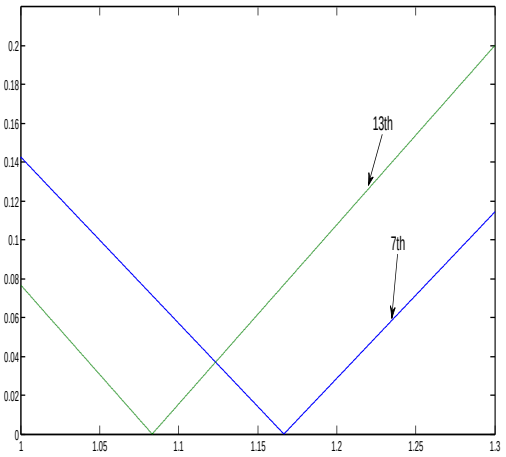

Figure (5) Sub-harmonic voltage induced by the positive sequence rotor current components related to the voltage induced by the fundamental component of the rotor current versus rotor angular per unit speed.

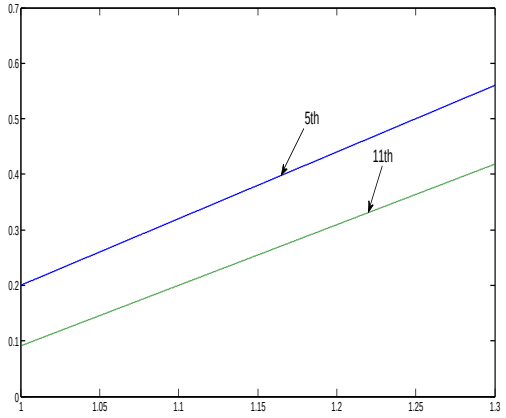

Figure (6) Sub-harmonic voltage induced by the negative sequence rotor current components related to the voltage induced by the fundamental component of the rotor current versus rotor angular per unit speed

The sub-harmonic voltages generated in the stator winding due to rotor harmonic currents (or magnetic fields)are calculated using the modified equivalent circuit of the DFIG shown in Fig.7 The voltage source $\mathbf{V_s}$ in the traditional equivalent circuit is replaced by a current source $\mathbf{V_s Y_s}$ in the modified equivalent circuit. The fundamental component of the rotor current ($\mathbf{I_f}$) referred to the stator side($\mathbf{I_f}/\sqrt{2}$ N)is represented also by a current source in the modified equivalent circuit.

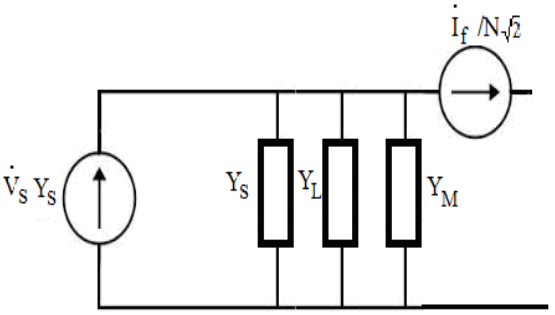

Figure (7) Modified equivalent circuit.

ISSN:2319-6890)(online),2347-5013(print)
01 Nov. 2015

The following basic equation for the currents in the circuit shown in Fig 7 can be written

$$\mathbf{V_s Y_s = E_1(Y_s + Y_m + Y_L) + I_f/\sqrt{2}\ N)} \quad (9)$$

Where $\mathbf{Y_s}$, $\mathbf{Y_m}$ and $\mathbf{Y_L}$ are the stator windings, magnetizing and load admittances simultaneously.

$\mathbf{I_f} = I_f\ (\cos\phi - j \sin\phi)$ (10)

N is the stator to rotor turns ratio

The ratio E_1/V_s can be easily calculated from equation (9) and multiplying this value by the RHS of either equation (7) or (8) and the sub-harmonic content E_h/V_s can be obtained.

The fundamental component of the rotor current (I_f) is calculated from the following equation [xv]:

$$(0.55\ I_f R_b + 0.605V_{oc})^2[1+3.21(1+s^2\beta^2)(\frac{R_r}{R_b})^2$$

$$-V_{oc}(0.55\ I_f R_b + 0.605V_{oc})[3.97(1+s^2\beta^2)(\frac{R_r}{R_b})^2 + 2.21\frac{R_r}{R_b}] \quad (11)$$

$$+1.2(1+s^2\beta^2)(\frac{R_r}{R_b})^2 V_{oc}^2 - s^2E_{2m}^2 = 0$$

and the angle

$$\phi = \arcsin[1.1(X_r/R_b)(1.54V_m/E_{2m} - V_{oc}/E_{2m}) \quad (12)$$

Where, s is the slip = $\frac{\omega_S - \omega}{\omega_S} = 1 - \nu$

$\beta = Xr / R_r$

R_r is the rotor resistance per phase in Ω

X_r is the rotor reactance per phase in Ω

E_{2m} is the maximum value of the rotor induced emf at stand-still in volts

V_{oc} is the battery pack open circuit voltage in volts

R_b is the internal resistance of the battery pack in Ω

The percentage of the sub-harmonics in the terminal voltage versus the rotor speed are shown in Figs (8) and (9) as calculated from the above equations for a DFIG whose data is given in the Appendix. The sub-harmonics created by the positive sequence harmonic rotor currents (7^{th}, and13^{th}) are given in Fig. (8).

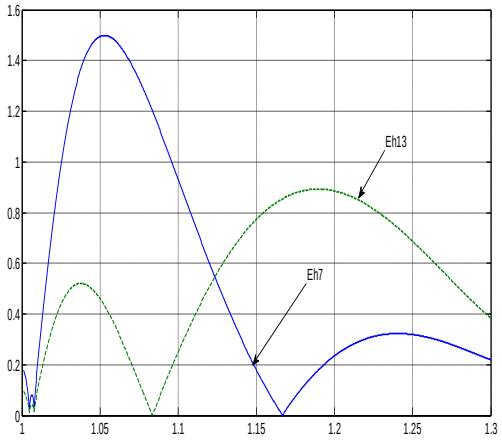

Figure (8) Percentage sub-harmonic components in the terminal voltage due to the 7^{th} & 13^{th} rotor current harmonics versus rotor angular per unit speed.

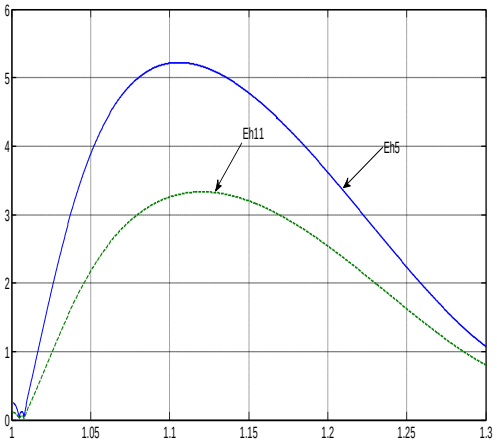

Figure (9) Percentage sub-harmonic components in the terminal voltage due to the 5^{th} & 11^{th} rotor current harmonics versus rotor angular per unit speed.

It is clear from Fig. (3) and Fig. (8) that the order of the sub-harmonics created by the 7^{th} harmonic in the rotor speed range ($1.3 > \nu > 1$) is always less than unity, i.e. the frequencies of these sub-harmonics voltages are less than the supply frequency. However, those created by the 13^{th} harmonic have frequencies ranging from the supply frequency to thrice the supply frequency. The characteristics of these sub-harmonics apply to any DFIG irrespective of its parameters.

Figure (8) shows the percentage of the sub-harmonic components created by the 7^{th} (less than 1.6%) and the 13^{th} (less than 1%) harmonic currents within the rotor speed range ($1 < \nu < 1.3$). These sub-harmonics become marginal (less than 1%) if the rotor speed is higher than the generator synchronous speed by 10% to 15%, i.e. ($1.1 < \nu < 1.20$).

The sub-harmonics created by the two negative sequence harmonic fields (5^{th} and 11^{th}), are demonstrated in Fig. (4) and Fig. (9). The order of the sub-harmonic fields created by the 5^{th} harmonic current ranges between first and third order while those created by the 11^{th} harmonic current ranges between first and fifth order as shown in Fig.(4).

The percentage of the sub-harmonic components created by the negative sequence fields (5^{th}, and11^{th}) may reach more than 6% of the terminal voltage when the rotor speed reaches 115% of the synchronous speed. These values do not exceed the IEC-61000 or EN-50160 standards limits.

In general, the order (or frequency) of the sub-harmonic voltage depend only on the rotor speed of the generator and the order (or frequency) of harmonic component of this rotor current that created it. However, this is not the case for the amplitudes of the sub-harmonic voltage which are functions of the generator parameters. The most influential parameter is the ratio of the rotor leakage reactance to the rotor resistance, β, [xv]. Figures 10, and 11 show the variation of the amplitudes of the sub-harmonic created by the 7^{th} 13^{th}, 5^{th} and 11^{th} harmonic currents with the rotor speed for two values of β (β= 15 and β=22.5).

It is clear from the calculated results that the amplitudes of the sub-harmonic voltage decrease with increase of β. This adds one more merit for the generators with greater values of β, i. e. better performance [xv] and less harmonics in the terminal voltage.

ISSN:2319-6890)(online),2347-5013(print)
01 Nov. 2015

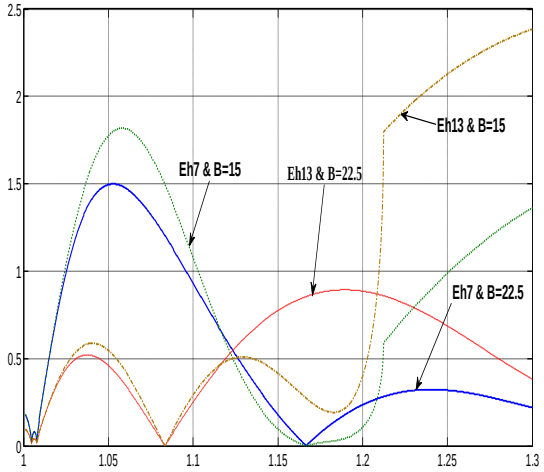

Figure (10) Percentage sub-harmonic components in the terminal voltage due to the 7th & 13th rotor current harmonics versus rotor angular per unit for two values of β (β= 15 and β=22.5).

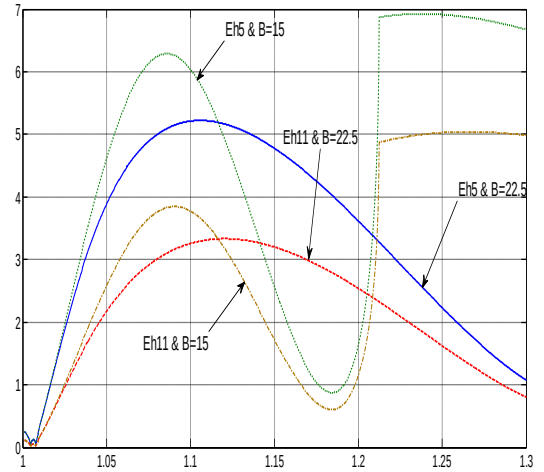

Figure (11) Percentage sub-harmonic components in the terminal voltage due to the 5th & 11th rotor current harmonics versus rotor angular per unit for two values of β (β= 15 and β=22.5).

IV. Conclusion

From the above mathematical analysis and results the following conclusions on the harmonics associated with the SM-BDFIG are drawn:

1. The harmonic components in the rotor current due to the presence of the 3-phase rectifier create sub-harmonics magnetic fields in the air gap of the SM-BDFIG.
2. The sub-harmonics magnetic fields rotate in space with varying speeds depending on the rotor angular speed and the order of the harmonic current component creating them.
3. The order or the per unit speed of each sub-harmonic magnetic field is not necessarily a multiple of the fundamental frequency. This sub-harmonic order may be a fraction or an integral number from the fundamental component.
4. The sub-harmonic fields induce sub-harmonics voltages in the stator windings. The order and the magnitude of the sub-harmonics voltages are functions of the rotor angular speed and of the order and magnitude of the harmonic current creating these sub-harmonic fields.
5. The stator terminal voltage is least affected by the positive sequence induced sub harmonics when the rotor speed range of operation is within 110% to 120% of the SM-BDFIG synchronous speed.
6. The negative sequence harmonic fields have increasing effect on the terminal voltage of the machine. However, the 110% to 120% of the SM-BDFIG super-synchronous speed range have acceptable impact according to the international standards.
7. It is recommended that during the design phase of the SM-BDFIG, the rotor speed corresponding to the prevailing wind speed (or rated wind speed), would be designed to lie in the range of 110% to 120% of the SM-BDFIG synchronous speed.
8. The generators with higher ratio of the rotor leakage reactance to the rotor resistance will have less impact of the sub-harmonics on its terminal voltage.

Appendix

Rated Power of the DFIG	1.5 MVA
Rated line to line voltage	0.69 kV
Number of poles	6
Rated frequency	60 Hz
Stator to rotor turns ratio	0.379
Stator winding resistance per phase	0.0016 Ω
Rotor winding resistance per phase	0.00464 Ω
Stator leakage reactance	0.0256 Ω
Rotor leakage reactance	0.1056 Ω
Magnetizing reactance	2.176 Ω
Angular moment of inertia	0.578 secs

References

i. *Mahmoud A. Saleh, and Mona N. Eskander, "A Single Machine Brushless DFIG for Grid-Connected and Stand-Alone WECS", British Journal of Applied Science & Technology, Volume No.4, Issue No.24, pp. 3550-3562, 2014, SCIENCE DOMAIN international, www.sciencedomain.org*

ii. Hopfenspergor B, Atkinson DJ, and Lakin RA. "Stator flux oriented control of a cascaded doubly-fed machine", IEE Electric Power Applications. Vol. 46, No. 6, 1999, pp: 597-605.

iii. Protesenke K, and Xu D. "Modeling and control of BDFIG in wind energy applications", IEEE Trans. Power Electronics, Vol. 23, No. 3, 2008, pp:1191-1197.

iv. Cardenas R, Pena R, and Clare J. "Control of a wind generation system based on brushless doubly-fed induction generator fed by a matrix converter", Electric Power Systems Research. Vol. 103, 2013, pp: 49-60.

v. Zhou D, Spec R, and Alexander GC. "Experimental evaluation of a rotor flux-oriented control algorithm for brushless doubly fed machine", IEEE Trans. Power Electronics, Vol. 12, 1997, pp: 72-78.

vi. Duro Basic, Jian Guo Zhu, and Gerard Boardmau. "Transient performance study of a brushless doubly fed twin stator induction generator", IEEE Trans. Energy Conversion, Vol. 18, No. 3, 2003 pp: 400-408.

vii. Ruviaro M, Runcos F, Sadowski N, and Borges IM. "Design and analysis of a brushless doubly induction machine with rotary transformer", International Conference of Electrical Machine, ICEM, Rome, Italy; 2010.

viii. Ruviaro M, and Runcos F. "A brushless doubly induction machine with flat plane rotary transformer", International Conference of Electrical Machine, ICEM, Marseille, France; 2012.

ix. Rahman Malik N, and Sadarangani C. "Brushless doubly induction machine with rotating power electronic converter for wind

ISSN:2319-6890)(online),2347-5013(print)
01 Nov. 2015

power applications", International Conference of Electrical Machine, ICEM, Beijing, China; 2011.

x. Yong Liao, Li Ran, Ghanim A. Putrus, and Kenneth S. Smith, "Evaluation of the Effects of Rotor Harmonics in a Doubly-Fed Induction Generator With Harmonic Induced Speed Ripple", IEEE Trans. on Energy Conversion, Vol. 18, No. 4, December 2003, pp: 508-518.

xi. Morgan Kiani, and Wei-Jen Lee, "Effects of Voltage Unbalance and System Harmonics on the Performance of Doubly Fed Induction Wind Generators", IEEE Trans. on Industry Applications, Vol. 46, No. 2, March/April 2010, pp: 562-569.

xii. Lingling Fan, Subbaraya Yuvarajan, and Rajesh Kavasseri, "Harmonic Analysis of a DFIG for a Wind Energy Conversion System", IEEE Trans. on Energy Conversion, Vol. 25, No. 1, March 2010, pp: 181-191.

xiii. Gidwani Lata and H.P. Tiwari, "Improving Power Quality of Wind Energy", Proceedings of International Multi-Conference of Energy Conversion Systems With Harmonic Fiters, IMECS 2011, March 16-18, 2011, HongKong.

xiv Changjin Liu, Frede Blaabjerg, Wenjie Chen, and Dehong Xu, "Stator Current Harmonic Control With Resonant Controller for Doubly Fed Induction Generator", IEEE Trans. on Power Electronics, Vol. 27, No. 7, July 2012, pp: 3207-3221

xv. Mahmoud A. Saleh, Maged N. F. Nashed, and Mona N. Eskander, "Steady State Analysis of Wind Driven SM-BDFIG in the Super-Synchronous Range of operation" International Journal of Engineering Research (IJER), Vol. 4, Issue 8, August 2015, pp: 412-418, www.ijer.in